Zinc(II) Complexes with Dimethyl 2,2'-Bipyridine-4,5-dicarboxylate: Structure, Antimicrobial Activity and DNA/BSA Binding Study

Tina P. Andrejević [1], Ivana Aleksic [2], Jakob Kljun [3], Bojana V. Pantović [1], Dusan Milivojevic [2], Sandra Vojnovic [2], Iztok Turel [3,*], Miloš I. Djuran [4] and Biljana Đ. Glišić[1,*]

[1] Department of Chemistry, Faculty of Science, University of Kragujevac, R. Domanovića 12, 34000 Kragujevac, Serbia; tina.andrejevic@pmf.kg.ac.rs (T.P.A.); pantovic.bojana@pmf.kg.ac.rs (B.V.P.)

[2] Institute of Molecular Genetics and Genetic Engineering, University of Belgrade, Vojvode Stepe 444a, 11042 Belgrade, Serbia; ivana_aleksic@imgge.bg.ac.rs (I.A.); dusan.milivojevic@imgge.bg.ac.rs (D.M.); sandravojnovic@imgge.bg.ac.rs (S.V.)

[3] Faculty of Chemistry and Chemical Technology, University of Ljubljana, Večna pot 113, SI-1000 Ljubljana, Slovenia; Jakob.Kljun@fkkt.uni-lj.si

[4] Serbian Academy of Sciences and Arts, Knez Mihailova 35, 11000 Belgrade, Serbia; milos.djuran@pmf.kg.ac.rs

* Correspondence: Iztok.Turel@fkkt.uni-lj.si (I.T.); biljana.glisic@pmf.kg.ac.rs (B.Đ.G.); Tel.: +386-1-47-98-525 (I.T.); +381-34-336-223 (B.Đ.G.)

Abstract: Two zinc(II) complexes with dimethyl 2,2'-bipyridine-4,5-dicarboxylate (py-2py) of the general formula [Zn(py-2py)X_2], X = Cl^- (**1**) and Br^- (**2**) were synthesized and characterized by NMR, IR and UV-Vis spectroscopy and single-crystal X-ray diffraction analysis. Complexes **1** and **2** are isostructural and adopt a slightly distorted tetrahedral geometry with values of tetrahedral indices τ_4 and τ'_4 in the range of 0.80–0.85. The complexes were evaluated for their in vitro antimicrobial activity against two bacterial (*Pseudomonas aeruginosa* and *Staphylococcus aureus*) and two fungal strains (*Candida albicans* and *Candida parapsilosis*), while their cytotoxicity was tested on the normal human lung fibroblast cell line (MRC-5) and the model organism *Caenorhabditis elegans*. Complex **1** showed moderate activity against both *Candida* strains. However, this complex was twofold more cytotoxic compared to complex **2**. The complexes tested had no effect on the survival rate of *C. elegans.* Complex **2** showed the ability to inhibit filamentation of *C. albicans*, while complex **1** was more effective than complex **2** in inhibiting biofilm formation. The interactions of complexes **1** and **2** with calf thymus DNA (ct-DNA) and bovine serum albumin (BSA) were studied to evaluate their binding affinity towards these biomolecules.

Keywords: zinc(II) complexes; pyridine-4,5-dicarboxylate esters; antimicrobial activity; cytotoxicity; anti-biofilm activity; DNA/BSA interaction

TABLE OF CONTENTS

Figure S1. C_{Ar}–H···Cl and C_{Ar}–H···Br interactions in complexes **1** and **2**. Selected distances (Å): (**1**) H6''-Cl1 2.761, H11-Cl2' 2.875, H12-Cl2'' 2.855, (**2**) H6''-Br2 2.851, H11-Br1' 3.010, H12-Br1'' 2.941. S4

Figure S2. ^{1}H NMR spectrum of complex **1** recorded in DMSO-d_6 at room temperature. S5

Figure S3. Time stability of complex **2** followed by UV-Vis spectrophotometry at room temperature in DMSO. S6

Figure S4. *C. elegans* under the microscope after 72 h of incubation with complexes **1** and **2** and the corresponding zinc(II) salts. S7

Figure S5. Filamentation of *C. albicans* ATCC 10231 in the presence of zinc(II) complex **2** (25 µg/mL), $ZnBr_2$ (25 µg/mL) and amphotericin B (1 µg/mL) in RPMI liquid medium (Olympus BX51, Applied Imaging Corp., San Jose, CA, United States, under 20 × magnification). S8

Figure S6. Inhibition of prodigiosin (a) and violacein (b) production in the presence of zinc(II) complexes **1** and **2**, and the corresponding zinc(II) salts tested on *Serratia marcescens* (a) and *Chromobacterium violaceum* CV026 (b) at 500 µg per disc concentration. S9

Figure S7. Fluorescence emission spectra of EthBr–DNA system in the presence of an increasing amount of complexes **1** (a) and **2** (b). The arrow shows the intensity changes upon the gradual addition of the complex. Inserted graph: Stern-Volmer plots of F_0/F vs. complex. S10

Figure S8. Photographs of single crystals of complexes **1** and **2**. S11

Table S1. Details of the crystal structure determination for complexes **1** and **2**. S12

Experimental data for dimethyl 2,2'-bipyridine-4,5-dicarboxylate (py-2py) S13

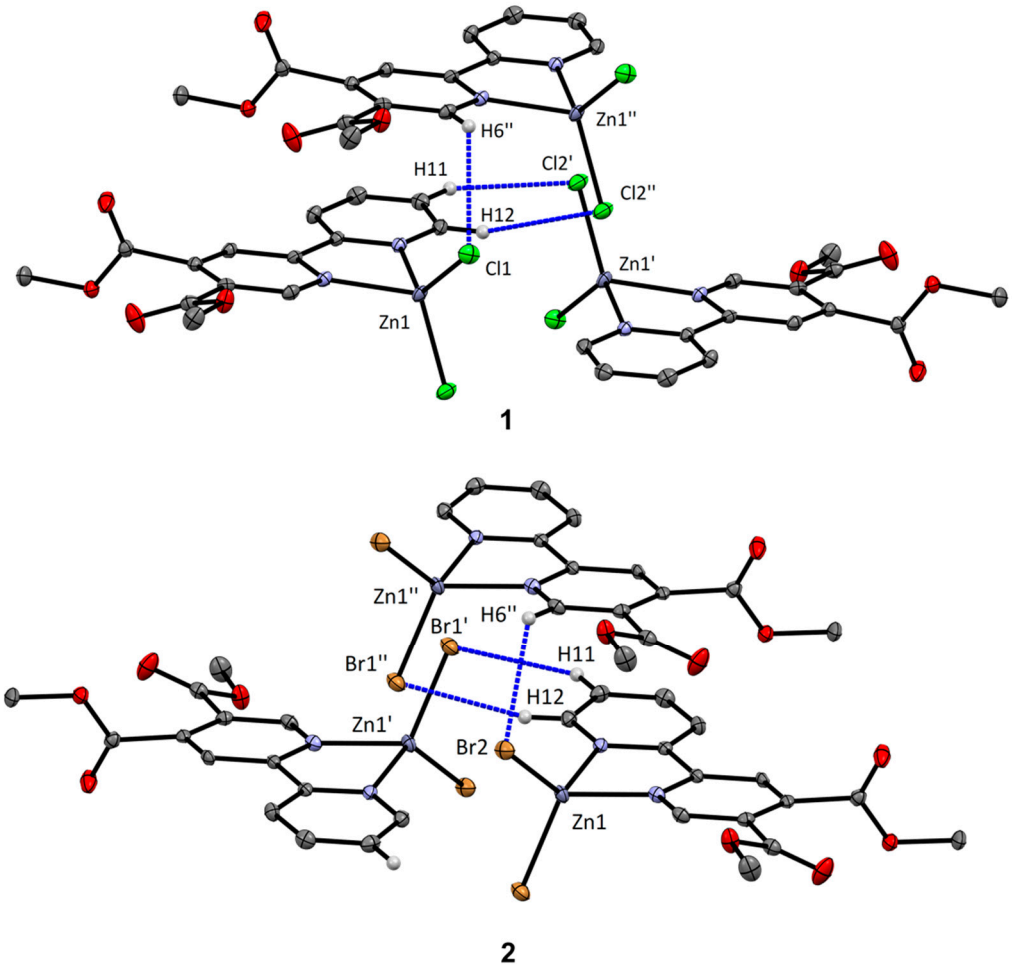

Figure S1. C_{Ar}–H···Cl and C_{Ar}–H···Br interactions in complexes **1** and **2**. Selected distances (Å): (**1**) H6''-Cl1 2.761, H11-Cl2' 2.875, H12-Cl2'' 2.855, (**2**) H6''-Br2 2.851, H11-Br1' 3.010, H12-Br1'' 2.941.

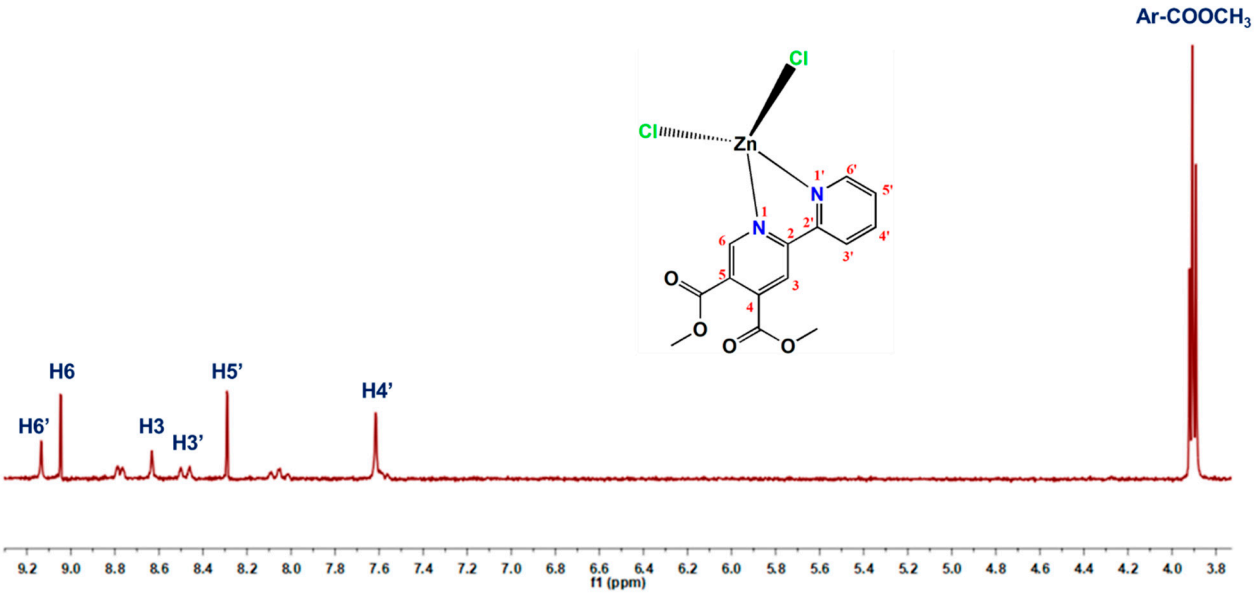

Figure S2. ^{1}H NMR spectrum of complex **1** recorded in DMSO-d_6 at room temperature.

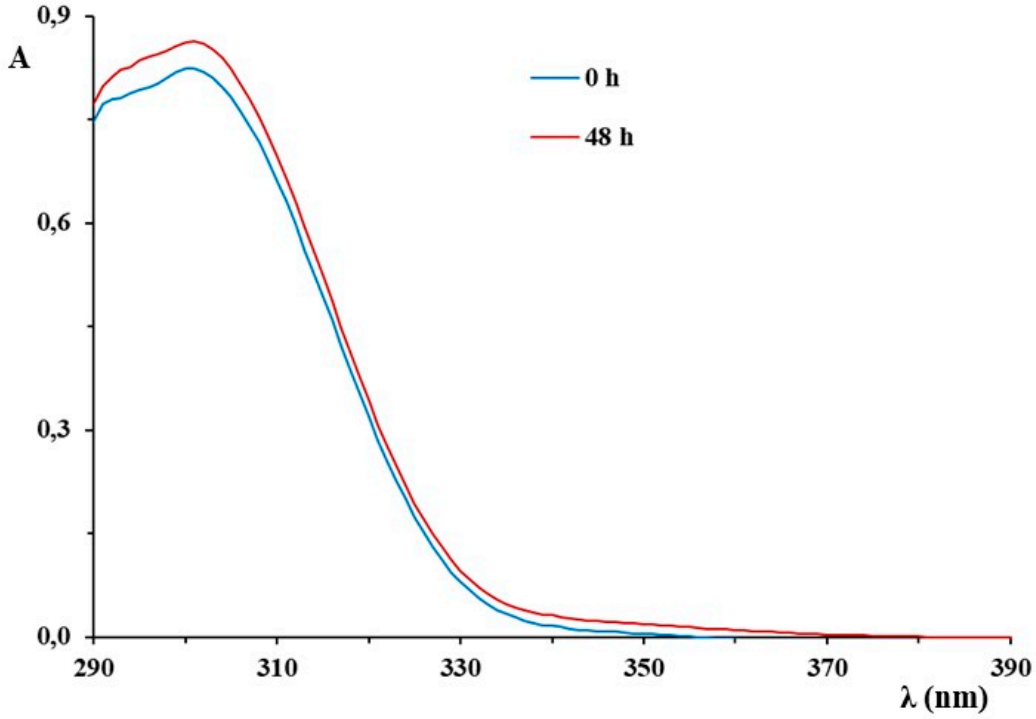

Figure S3. Time stability of complex **2** followed by UV-Vis spectrophotometry at room temperature in DMSO.

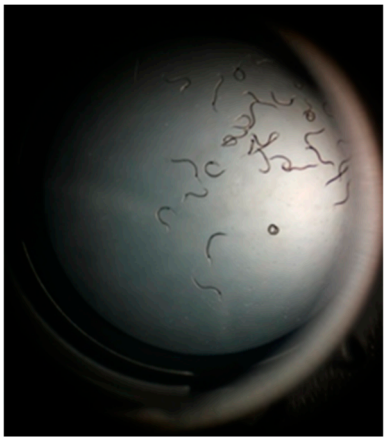

Figure S4. *C. elegans* under the microscope after 72 h of incubation with complexes **1** and **2** and the corresponding zinc(II) salts.

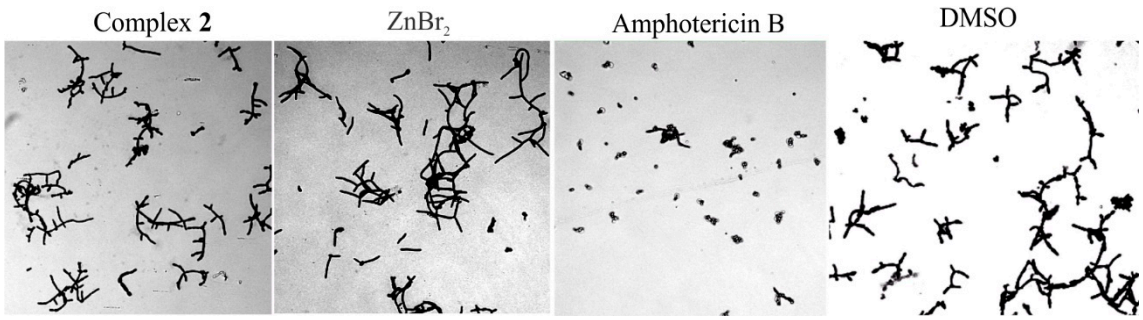

Figure S5. Filamentation of *C. albicans* ATCC 10231 in the presence of zinc(II) complex **2** (25 μg/mL), $ZnBr_2$ (25 μg/mL) and amphotericin B (1 μg/mL) in RPMI liquid medium (Olympus BX51, Applied Imaging Corp., San Jose, CA, United States, under 20 × magnification).

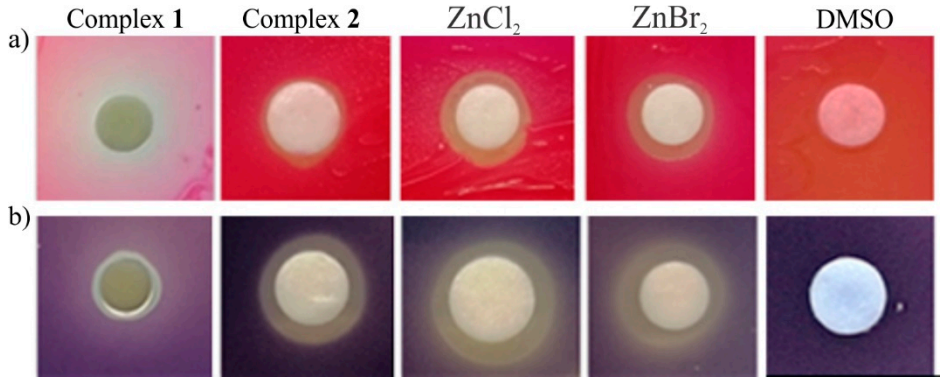

Figure S6. Inhibition of prodigiosin (a) and violacein (b) production in the presence of zinc(II) complexes **1** and **2**, and the corresponding zinc(II) salts tested on *Serratia marcescens* (a) and *Chromobacterium violaceum* CV026 (b) at 500 μg per disc concentration.

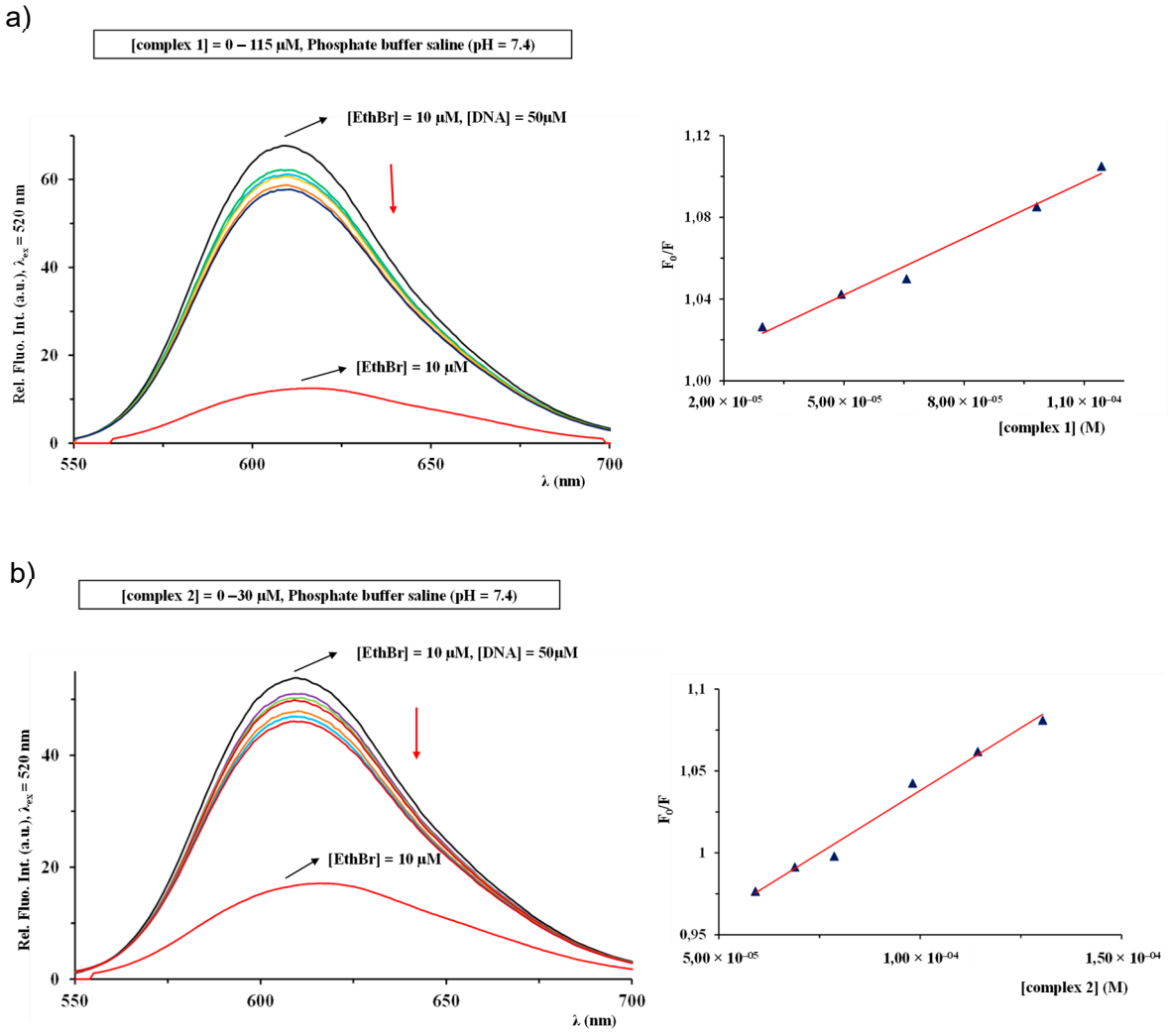

Figure S7. Fluorescence emission spectra of EthBr–DNA system in the presence of an increasing amount of complexes **1** (a) and **2** (b). The arrow shows the intensity changes upon the gradual addition of the complex. Inserted graph: Stern-Volmer plots of F_0/F vs. complex.

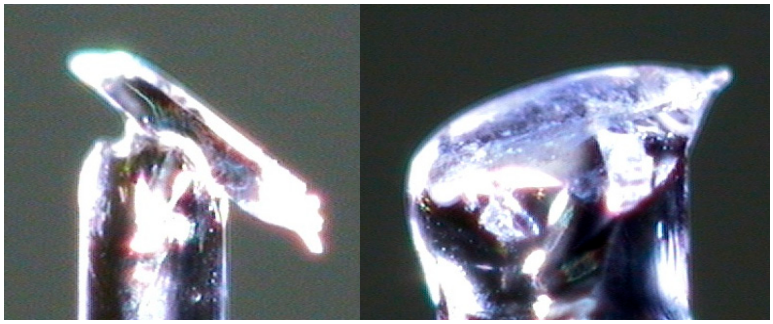

1 **2**

Figure S8. Photographs of single crystals of complexes **1** and **2**.

Table S1. Details of the crystal structure determination for complexes **1** and **2**.

Compound	**1**	**2**
CCDC No.	2162358	2162359
Empirical formula	$C_{14}H_{12}Cl_2N_2O_4Zn$	$C_{14}H_{12}Br_2N_2O_4Zn$
Formula weight	408.53	497.45
Temperature [K]	150.00(10)	150.00(10)
Crystal system	monoclinic	monoclinic
Space group	*I*2/a	*I*2/a
a [Å]	16.9633(5)	17.3072(6)
b [Å]	5.1483(2)	5.1940(2)
c [Å]	35.7066(9)	36.0564(12)
α [°]	90	90
β [°]	90.557(2)	90.665(3)
γ [°]	90	90
Volume [$Å^3$]	3118.19(17)	3241.0(2)
Z	8	8
ρ_{calc} [g/cm^3]	1.740	2.039
μ [mm^{-1}]	1.938	6.467
F(000)	1648.0	1936.0
Crystal size [mm^3]	0.5 × 0.5 × 0.3	0.3 × 0.3 × 0.03
Radiation	Mo Kα (λ = 0.71073)	Mo Kα (λ = 0.71073)
2Θ range for data collection [°]	5.338 to 54.964	4.708 to 58.68
Index ranges	$-22 \le h \le 20$, $-6 \le k \le 5$, $-45 \le l \le 46$	$-23 \le h \le 16$, $-5 \le k \le 6$, $-49 \le l \le 47$
Reflections collected	10560	10656
Independent reflections	3569 [R_{int} = 0.0187, R_{sigma} = 0.0185]	3881 [R_{int} = 0.0542, R_{sigma} = 0.0543]
Data/restraints/parameters	3569/0/210	3881/0/210
Goodness-of-fit on F^2	1.046	1.028
Final R indexes [$I \ge 2\sigma(I)$]	R_1 = 0.0216, wR_2 = 0.0559	R_1 = 0.0383, wR_2 = 0.0879
Final R indexes [all data]	R_1 = 0.0240, wR_2 = 0.0570	R_1 = 0.0522, wR_2 = 0.0955
Largest diff. peak / hole [$e/Å^3$]	0.36/-0.24	0.98/-0.73

Experimental data for dimethyl 2,2'-bipyridine-4,5-dicarboxylate (py-2py)

IR (KBr, ν, cm^{-1}): 3065w, 3004w ($\nu(C_{ar}–H)$), 2951w (ν(C–H)), 1734vs, 1718vs (ν(C=O)), 1599w, 1585m, 1569w, 1549m, 1460m, 1439s, 1426m ($\nu(C_{ar}=C_{ar})$) and ($\nu(C_{ar}=N)$), 1297vs, 1282vs (ν(C–O)), 785s ($\gamma(C_{ar}–H)$). ^{1}H NMR (500 MHz, DMSO-d_6): δ = 3.92 (*d*, *J* = 7.7 Hz, 6H, Ar-$COOCH_3$), 7.61 (*ddd*, *J* = 7.6, 4.8, 1.2 Hz, 1H, H4'), 8.06 (*td*, *J* = 7.8, 1.8 Hz, 1H, H5'), 8.49 (*dt*, *J* = 8.0, 1.1 Hz, 1H, H3'), 8.63 (*d*, *J* = 0.8 Hz, 1H, H3), 8.78 (*ddd*, *J* = 4.8, 1.8, 0.9 Hz, 1H, H6), 9.14 (*d*, *J* = 0.8 Hz, 1H, H6') ppm. UV-Vis (DMSO, λ_{max}, nm): 300.0 ($\varepsilon = 1.3 \times 10^4$ $M^{-1}cm^{-1}$).